Eur. Phys. J. B **52**, 155–162 (2006)
DOI: 10.1140/epjb/e2006-00283-9

THE EUROPEAN PHYSICAL JOURNAL B

A new handshaking of Tight-Binding and Molecular Dynamics in multi-scale simulation

L.S. Pan[a], X.H. Wu, D. Xu, C. Lu, and H.P. Lee

Institute of High Performance Computing, 1 Science Park Road, #01-01 The Capricorn Singapore Science Park II, Singapore 117528, Singapore

Received 25 January 2006 / Received in final form 17 May 2006
Published online 11 July 2006 –

Abstract. A new handshake scheme is presented for tight-binding (TB) and molecular dynamics (MD) for multi-scale simulation of covalent crystals. In the present scheme, when calculating the forces on MD atoms in the handshake region, the TB atoms in close proximity to the MD atoms are treated as MD atoms. The scheme is thus seamless for calculation of MD atoms. When determining the electronic states of the TB subsystem, instead of the four basic atomic orbitals, hybrid orbitals are employed as bases in TB method and also as representing the action of MD atoms on TB atoms. The present handshaking methodology has several advantages. Firstly, it avoids determining the physical parameters required by introducing a new orbital model. Secondly, the "seam" almost decreases by one order of magnitude compared to that of Silogen model. Thirdly, the whole scheme is stable for dynamic simulation.

PACS. 71.15.Pd Molecular dynamics calculations (Car-Parrinello) and other numerical simulations – 46.50.+a Fracture mechanics, fatigue and cracks

1 Introduction

With the rapid development of material science, the simulation techniques are expected to be capable of capturing the phenomena occurring at micro-scales. For example, phenomena involving crack tip propagation in materials and connection of two materials are all at nano/micro-order of magnitude in scale. For the simulations of physical phenomena with microscopic characteristics, the numerical methods based on molecular dynamics (MD) have to be applied. Various MD simulation methods have been developed. Their successful applications can be seen from some reported studies [1–6].

It is well know, however, that for the accurate description of microscopic physical phenomena, quantum mechanical theory is more precise than molecular dynamics models. Based on this fact, Abraham et al. [7–9], Broughton et al. [10], Rudd et al. [11] and Nernstern [12] recently developed a new multi-scale method. Instead of molecular dynamics, they introduced quantum tight binding (TB) approximation to describe the crack propagation in a very small region close to the crack tip. For the region far away from the crack tip, the finite element (FE) technique, based on the continuum approximation, is still applied to simulate the large-scale elastic field. The MD model is taken as the bridge between TB and FE. Their ideal is of great significance for numerical simulations. Firstly, the quantum description of atomic bonding at the crack tip is more accurate than the molecular dynamics description. Secondly, besides crack problem, the method can be used to simulate the other properties of materials. Thirdly, the combination of TB and MD can also serve as a useful numerical tool for prediciting the behavior of various nano-materials.

However since different theoretical models are used in different subsystems, physical information in the handshake of the two subsystems may have a seam. This seam will directly influence the accuracy of numerical results. Therefore research for a reasonable handshaking methodology is one of key consideration for such a mulit-scale simulation; as said by Broughton et al. [10], "once the handshakes are made 'seamless', the algorithm is not only efficient, it is also very accurate". Abraham and his coworkers [10] discussed in detail handshaking between TB and MD for the fracture problem of covalent bond crystal, Si. In their handshaking scheme between TB and MD, some univalent "silogens" similar to hydrogen atoms are introduced acting on the outer perimeter of the TB region. These silogens are constrained to sit at the positions occupied by the MD atoms adjacent to the TB atoms and thus play a role of mutual influence between TB and MD regions. Ogata et al. [13] presented another handshaking between density function theory and MD in 2002, where all the termination hydrogen atoms (similar to the above silogen) are not at the positions occupied by MD atoms. The positions of the termination hydrogens are chosen to

[a] e-mail: panls@ihpc.a-star.edu.sg

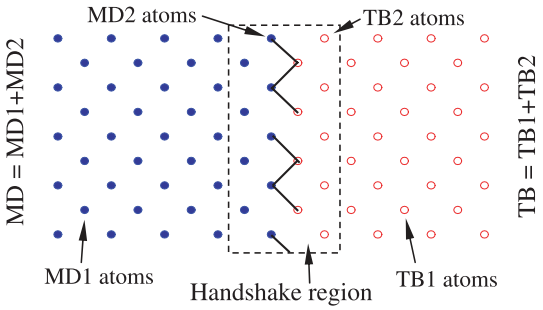

Fig. 1. Illustration of MD/TB handshake.

minimize the mean square forces on all atoms in the quantum system. This procedure requires a considerable computational effort for dynamic simulations.

In this paper, a new handshake scheme for TB/MD multi-scale dynamic simulation is presented for covalent bond crystals. The paper is organized as follows. In Section 2, MD and TB schemes are described briefly. The difference between the basic atomic state for TB atoms in the present and existing schemes are highlighted (for convenience, Abraham et al.'s scheme [10] is called the silogen-scheme in the present paper). The new handshaking between TB and MD is introduced in Section 3 and in Section 4 the numerical verification of the present scheme is discussed. Finally concluding remarks are given in Section 5.

2 Brief descriptions on MD and TB schemes

For the convenience of introducing the new handshake scheme, we separately describe the main concepts behind the MD and TB dynamic simulations. A more detailed description can be found in the reported studies [7–12].

Let us consider a system comprising of N atoms initially at positions $\{\mathbf{r}_i | i = 1, ...,N\}$. Suppose N_1 atoms in the right side of this system to be simulated by the tight binding approximation and the remainder on the left by molecular dynamics technique based on empirical potential (as shown in Fig. 1).

For the MD atoms, the Stillinger-Weber [14] (SW) potential,

$$V_{SW} = \sum_{i<j} V^{(2)}(r_{ij}) + \sum_{i,(j<k)} V^{(3)}(r_{ij}, r_{ik}), \qquad (1)$$

is chosen as their mutual action potential and the force $\boldsymbol{F}_i^{\mathrm{MD}}$ on the ith MD atom is calculated by means of,

$$\mathbf{F}_i^{\mathrm{MD}} = -\frac{\partial V_{SW}}{\partial \mathbf{r}_i}, \qquad (2)$$

where $r_{\mathrm{ij}} = |\boldsymbol{r}_{\mathrm{ij}}| = |\boldsymbol{r}_{\mathrm{j}} - \boldsymbol{r}_i|$ and the sums are over all the MD atoms. The velocity-Verlet algorithm is chosen as the integrator for Newton's law of motion as it is a simply implemented explicit scheme with high accuracy for a given time step.

For the TB atoms, the total energy is comprised of two parts as follows

$$V_{TB} = \sum_{n=1}^{N_{\mathrm{occ}}} E_{\mathrm{n}} + \sum_{i<j} V_{\mathrm{rep}}(\boldsymbol{r}_{ij}). \qquad (3)$$

Here E_{n} is the energy of nth eigenstate $|\Psi_{\mathrm{n}}\rangle$ under the one-electron approximation to the first principles; N_{occ} is the number of occupied states of electronic system up to the Fermi-level; V_{rep} stands for inter-atomic repulsive potential. The energy E_{n} is obtained by solving the following time-independent Schroedinger equation,

$$\mathbf{H}|\Psi\rangle = E|\Psi\rangle, \qquad (4)$$

where $\boldsymbol{H}$ is the Hamiltonian under the one-electron approximation. To solve this equation, the electronic wave function Ψ is expanded into the linear combination of some basis functions,

$$|\Psi\rangle = \sum_{i=1}^{N_1}\sum_{\alpha=1}^{N_\alpha} c_{i\alpha}|\psi_{i\alpha}\rangle + \sum_{l=1}^{L} c_l|\psi_l\rangle, \qquad (5)$$

where $|\psi_{i\alpha}\rangle$ stands for the αth atomic orbitals on the ith TB atom; ψ_l is the orbital wave function reflecting the effect of MD atoms on the TB atoms and L is the number of such wave functions; $C_{i\alpha}$ and C_l are the coefficient to be determined; N_α is the number of covalent bonds (or covalent electrons) of an atom in crystal and changes with the structure of covalent crystal. For example, N_α is 4 in the diamond crystals.

Traditionally, the four basic orbitals, s, p_x, p_y and p_z, are directly taken as $\psi_{i\alpha}$ as done in the reference [10]. In the present scheme, however, instead of these four basic orbitals, the hybrid orbitals are chosen as $\psi_{i\alpha}$ in (5) because they are capable of reflecting the orientation of covalent bond. For example, if the hybrid orbital is formed by s- and/or p-electrons, then

$$|\psi_{i\alpha}\rangle = \alpha_s|s_i\rangle + \alpha_x|p_{ix}\rangle + \alpha_y|p_{iy}\rangle + \alpha_z|p_{iz}\rangle \qquad (6)$$

where $(\alpha_x, \alpha_y, \alpha_z)$ stands for the orientation of hybrid orbital and $\alpha_s^2 + \alpha_x^2 + \alpha_y^2 + \alpha_z^2 = 1$. The method of determining these coefficients can be found in hybrid bond theory or structure chemistry. As the second term in the right hand side of equation (5) represents the effect of electrons of MD atoms on the TB atoms. How to choose the electronic wave function ψ_l is one of keys for handshaking between the TB and MD atoms. A detailed discussion will be presented in the next section.

Substituting equations (5) and (6) into equation (4) and utilizing the variational principle, we can obtain a set of algebraic eigenvalue equations for the energy E and the coefficients in equation (5)

$$\left[\begin{pmatrix} H_{\mathrm{II}} & H_{\mathrm{IL}} \\ H_{\mathrm{LI}} & H_{\mathrm{LL}} \end{pmatrix} - E\begin{pmatrix} S_{\mathrm{II}} & S_{\mathrm{IL}} \\ S_{\mathrm{LI}} & S_{\mathrm{LL}} \end{pmatrix}\right]\begin{pmatrix} C_{\mathrm{I}} \\ C_{\mathrm{L}} \end{pmatrix} = 0 \qquad (7)$$

where $(C_{\mathrm{I}}, C_{\mathrm{L}})$ have the form,

$$\left.\begin{aligned} (C_{\mathrm{I}})^+ &= (c_{11}, c_{12}, c_{13}, c_{14}, c_{21}, \cdots\cdots) \\ (C_{\mathrm{L}})^+ &= (c_1, c_2, c_3, c_4, c_5, \cdots\cdots) \end{aligned}\right\}. \qquad (8)$$

The subscript 'I' here is equal to $N_\alpha \times N_1$. In order to more clearly show the influence of MD atoms on the TB atoms, Hamitonian matrix H and non-orthogonal matrix S (due to applying non-orthogonal orbital model) are separately expressed into four sub-matrices, $H_{\rm II}$, $H_{\rm IL}$, $H_{\rm LI}$, $H_{\rm LL}$, $S_{\rm II}$, $S_{\rm IL}$, $S_{\rm LI}$ and $S_{\rm LL}$. The effect of MD atoms on TB atoms is represented through $H_{\rm IL}$, $H_{\rm LI}$, $S_{\rm IL}$ and $S_{\rm LI}$. Further discussion of H and S matrices is provided in the appendix.

Applying the eigen-energies $E_{\rm n}$ and the corresponding normalized coefficients obtained through solving equation (7), the force acting on the ith TB atom can be deduced by differentiating expression (3).

$$\mathbf{F}_i = -\sum_{n=1}^{N_{\rm occ}} (C_{\rm I}^n C_{\rm L}^n) \left[\begin{pmatrix} \frac{\partial H_{\rm II}}{\partial \boldsymbol{r}_i} & \frac{\partial H_{\rm IL}}{\partial \boldsymbol{r}_i} \\ \frac{\partial H_{\rm LI}}{\partial \boldsymbol{r}_i} & \frac{\partial H_{\rm LL}}{\partial \boldsymbol{r}_i} \end{pmatrix} - E_n \begin{pmatrix} \frac{\partial S_{\rm II}}{\partial \boldsymbol{r}_i} & \frac{\partial S_{\rm IL}}{\partial \boldsymbol{r}_i} \\ \frac{\partial S_{\rm LI}}{\partial \boldsymbol{r}_i} & \frac{\partial S_{\rm LL}}{\partial \boldsymbol{r}_i} \end{pmatrix} \right] \begin{pmatrix} C_{\rm I}^n \\ C_{\rm L}^n \end{pmatrix} - \sum_{j \neq i} \frac{\partial V_{rep}(r_{ij})}{\partial \boldsymbol{r}_i}. \quad (9)$$

After calculating the forces acting on each TB atom, the classical paths of the atoms can then be determined.

3 Handshaking between TB and MD atoms

In the previous section, a system of atoms under consideration is artificially divided into MD and TB subsystems as shown in Figure 1 and the different physical models are applied to the subsystems. This will give rise to a "seam" of physical quantities (such as forces acting on atoms) appearing at handshake atoms of the two subsystems. To ensure the availability of TB-MD multi-scale simulation, the "seam" of a numerical scheme must be sufficiently small.

First, let's discuss the simulation of MD atoms. The action radius of the SW potential function is around 1.6 times the length of a bond, an MD atom will not experience any force from particles outside of this radius. Hence, when the handshake region (see Fig. 1) is chosen to be suitably wide, the MD1 atoms (MD atoms outside the handshake region) will not be acted upon by the TB atoms. The MD2 atoms will be affected by the TB2 atoms in the handshaking zone. However, if the SW potential, rather than tight binding approximation, is used to calculate the action of the TB2 atoms on the MD2 atoms, the environment of MD1 and MD2 atoms will be the same as an identical potential function is applied to all of the MD atoms.

It can be seen from the above discussion that for the MD subsystem it does not need to distinguish MD1 atoms from MD2 atoms. The identical formulas (1) and (2) can be applied to compute the forces acting on the all MD atoms as if the whole system was not divided in the MD and TB subsystems. The inconsistency of a dynamic description of the MD atoms can be avoided by eliminating the artificial subdivision of the system into TB and MD regions. Therefore the present computational scheme for the MD subsystem is almost seamless.

Now, we turn to the TB subsystem. Equation (9) shows that force acting on a TB atom originates from two parts, the inter-atomic repulsive potential and summation over all occupied one-electron energy-states. It can be seen from equation (3) that the repulsive potential in tight binding approximation is also only dependent on relative positions among atoms and the cut-off radius is small. The repulsive potential and molecular potential are thus similar in the type of functions. Hence the above treatment on MD atoms can be used directly to calculate the repulsive force. Specifically, when computing the repulsive forces exerted on TB2 atoms inside the handshake region, the MD2 atoms are regarded as the 'TB' atoms as if the whole system consists of the TB atoms, although the motion of MD2 atoms is determined by molecular dynamics model (or SW potential). Clearly, the repulsive force obtained by such computation should be seamless from TB1 to TB2 atoms.

The other part of force originating from summating energy of all one-electron states is the major part of force on a TB atom. The discussion from equations (3) to (9) has shown that this part of force depends strongly on the chosen atomic orbital ψ_l reflecting the effect of MD atoms on the TB atoms. The key of decreasing the 'seam' between the TB and the MD atoms is thus to reasonably choose and treat the atomic orbital ψ_l.

Traditionally, all ψ_l in equation (5) are taken as one type, i.e., s-like orbital similar to hydrogen. For instance, "silogen" model introduced in references [7–12] belongs to this type. These researchers brought forward 4 or 5 requirements to determine the physical parameters of the silogen model. The purpose of these requirements is to maintain as much of the bond structure properties of covalent crystal as possible in the connection of the MD and TB atoms. It has been mentioned in the previous section that for most covalent crystals, the hybrid atomic orbitals better reflect the bonding structure among atoms. Hence in the present scheme, instead of the isotropic s-like orbital, the hybrid atomic orbital itself is chosen as $|\psi_l\rangle$ in equation (5). In other words, like the previous procedures on the SW potential and the repulsive potential, those MD2 atoms close to the TB2 atoms are first regarded as TB atoms (for the convenience of discussion below, they are called MDT atoms). Thus each MDT atom has the same hybrid orbitals as the TB atoms, as shown in expression (6). Some of the hybrid orbitals are then selected as $|\psi_l\rangle$ in equation (5) and is moved with the corresponding MDT atom. It should be noted that the chosen hybrid orbitals may change form MDT atom to MDT atom.

It is well known that a TB atom may have several hybrid orbitals. The orientation of orbitals determines which hybrid orbital is most suitable for a given MDT. If the orientation of a hybrid orbital is towards the TB subsystem (region), this hybrid orbital must be selected for the MDT atom. For instance, a silicon atom in a diamond structure has 4 hybrid orbitals: $|\psi_{i1}\rangle$, $|\psi_{i2}\rangle$, $|\psi_{i3}\rangle$ and $|\psi_{i4}\rangle$, and each one has its special orientation in crystal. If the

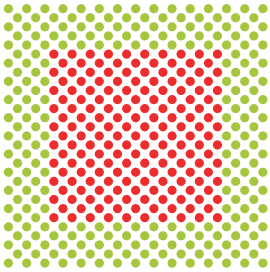

Fig. 2. A part of simulated silicon atoms as viewed from z-direction.

orientations of orbitals $|\psi_{i1}\rangle$ and $|\psi_{i3}\rangle$ of a MDT atom point to the TB subsystem, both of these hybrid orbitals are then chosen as $|\psi_l\rangle$.

The orbital $|\psi_l\rangle$ chosen at present is in the same type with $|\psi_{i\alpha}\rangle$ of the internal TB atoms. It can thus interact with any TB2 atom only when it is sufficiently close to the center of $|\psi_l\rangle$. When calculating the values of matrix elements in equation (7), it is not necessary to make any special procedure on the matrix elements involving $|\psi_l\rangle$.

The above discussion has detailed the main advantages of the new handshkaing regime. Firstly, it avoids the trouble of computing the physical parameters needed in any hydrogen-like model due to the present $|\psi_l\rangle$ being constructed by linear superposition of the four basic atomic orbitals. Thus the various physical parameters required by the hybrid orbital can be obtained directly from the basic orbitals without requiring any further numerical calculation. For example, the orbital energy of $|\psi_l\rangle$ is $\alpha_s^2 E_s + (\alpha_x^2 + \alpha_y^2 + \alpha_z^2)E_p$, where E_s and E_p are the energies of s- and p-orbitals, respectively. Secondly, each $|\psi_l\rangle$ is not limited to act on only a given TB atom. When the system is at a state of equilibrium, $|\psi_l\rangle$ naturally acts on only one TB atom located at the oriented axis of $|\psi_l\rangle$ as the two-center integral values between it and the orbitals of other TB atom are zero. However, when the system is at dynamic state, it is reasonable to assume that the two-center integral values between $|\psi_l\rangle$ and the orbitals of more TB atoms are non-zero. Third, the present $|\psi_l\rangle$ is of the same type as $\psi_{i\alpha}$ for the pure TB atoms. Thus, the TB atoms within the handshaking zone have an almost consistent interaction with the pure TB atoms, resulting in a narrow "seam". The numerical verification of this procedure will be given in the next section. Finally, the present ψ_l is a more realistic representation of the interaction between the MD and the TB atoms. This is because the hybrid bond itself can be viewed as the connecting bond between two atoms in the covalent crystal.

4 Numerical verification and discussion

For verification and comparison, the present and the existing handshake schemes are applied to compute the forces acting on every atom in silicon slab with diamond structure. Figure 2 shows a part of the simulated silicon atoms as viewed from the z-direction normal to the plane. The red region stands for TB silicon atoms and the green region represents MD silicon atoms. Outside the figure are all the MD atoms. For the MD atoms, the SW potential is used and for the TB atoms the NO-TB model provided by Bernsterin and Kaxiras [15] is applied. In the present computation, a periodic boundary condition is applied in the z-direction and the period is the length of two crystal lattices. To decrease the cut-off error, the double precision computation is used.

Figure 3 shows the distribution of inter-atomic forces along the atoms in a primary cell layer in the z-direction. These atoms are assumed to locate at ideal crystal lattices under the zero temperature. For the convenience of observing and comparing the forces, the atoms inside the layer are drawn in a horizontal plane although they have different z-coordinates. It should be noted that all quantities are dimensionless. The characteristic parameters, which are used to make variables dimensionless, are the energy of the s-electron, the bond length at zero temperature and the atomic mass.

It is well known that the when atoms are at equilibrium positions, the total force exerted on each atom is zero. Figure 3 exhibits clearly that the forces on the MD atoms and the TB atoms outside handshake region are indeed almost zero, but the forces on the TB2 atoms inside the region are not. This indicates that the two types of handshaking will all give rise to error (or seam) of the action force on TB2 atoms. It can be observed from this figure that the errors of the two handshake schemes are not of the same order of magnitude. In Figures 3a-(1, 2), the maximum force along the TB atoms is about 0.1 while in Figure 3b-(1, 2), the maximum value is about 0.018. It implies that the present scheme reduces the error by 80% relative to the old scheme. By comparison with Figures 3a-(1, 2), Figure 3(a, 3) shows that the error for the z-component of force is also relatively small. This may be due to the application of periodic condition in the z-direction. But it can also be seen from Figure 3(b, 3) that the error of the present scheme is smaller in this direction.

Besides the magnitude of error in ideal crystal state, another criterion of assessing a handshaking scheme is the stability of the scheme. If the error decreases as time progresses, the scheme is stable and usable. This is very important for dynamic simulation. For this purpose, the case mentioned above without any external force action is dynamically simulated. Dimensionless time step taken here is $\Delta t = 0.01$.

For the present scheme, two things are found from the numerical simulation. First, the seam along TB boundary atoms gradually becomes smaller and smaller as time advances, and ultimately disappears. This fact can be seen in Figure 4. Figure 4a shows that there is a distributed force (seam) along the TB boundary atoms at $t = 0$. After undergoing 3000 time steps, the seam can no longer be observed in Figure 4b. Instead, there is a very small force on every MD and TB atom. Second, all the MD and the TB atoms vibrate with very small amplitudes after 500 time steps. Figure 4b implies that almost all atoms are away from their equilibrium positions.

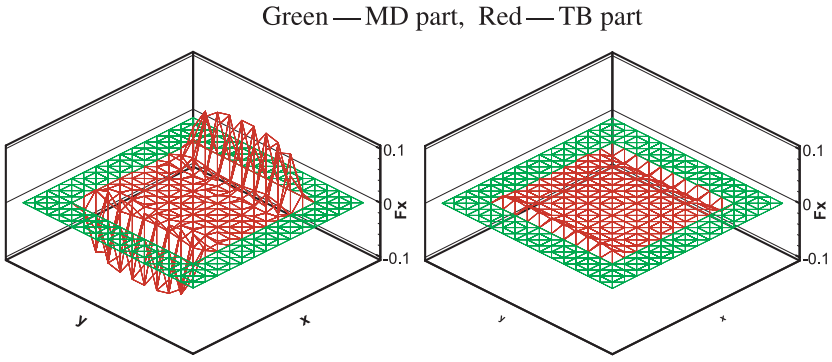

(**a**-1) (**b**-1)

Distribution of the x-component force among atoms.

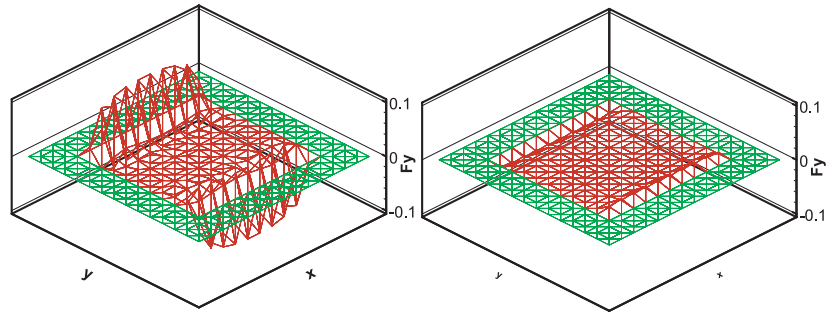

(**a**-2) (**b**-2)

Distribution of the y-component force among atoms.

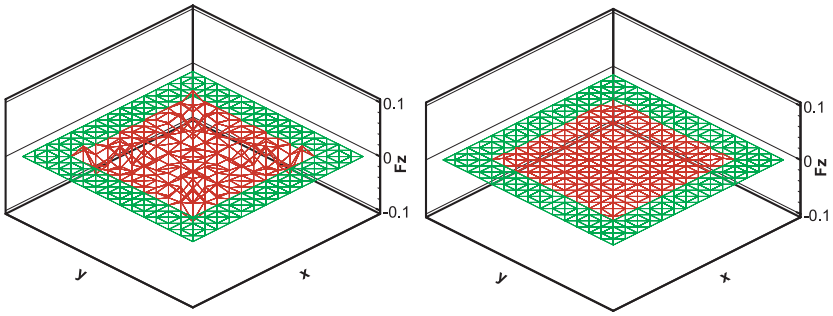

(**a**-3) (**b**-3)

Distribution of the z-component force among atoms.

Fig. 3. Comparison of inter-atomic forces computed by two handshakes: **(a)** old scheme, (**b**) present scheme.

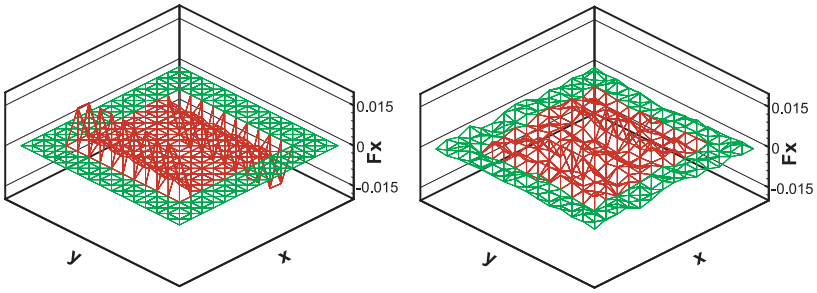

(a: $t = 0$) (b: $t = 3000\ \Delta t$)

Fig. 4. Change of force-seam from $t = 0$ to $3000\Delta t$.

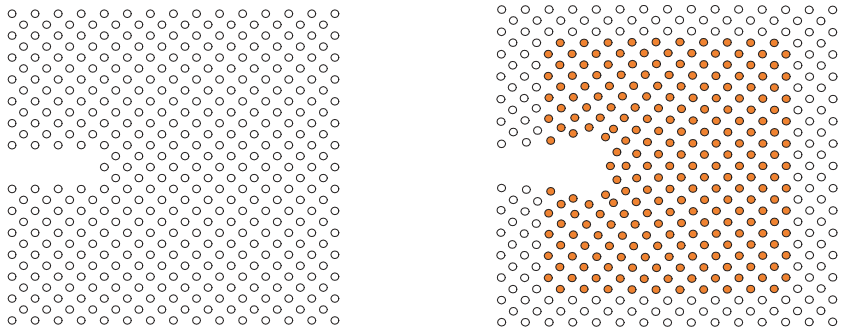

(**a:** $t = 0$) (**b:** $t = 500\ \Delta t$)

Fig. 5. Evolution of crack tip in Si material with diamond structure (black circles — MD atoms, red solid circles — TB atoms).

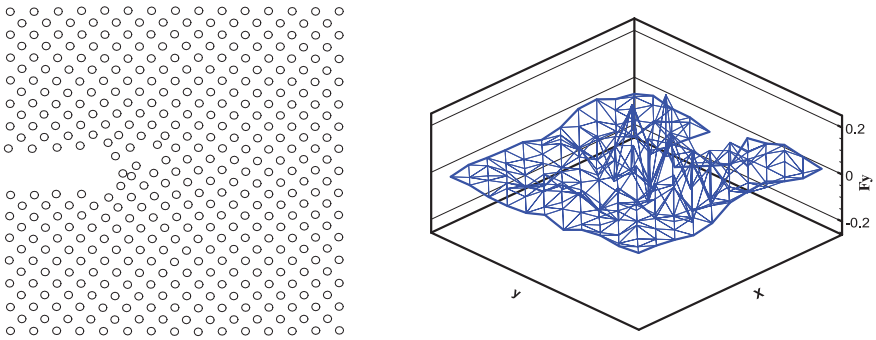

(**a:** after tension for $t = 8000\Delta t$) (**b:** y-component force among atoms)

Fig. 6. The configuration of crack tip and the force on atoms at the instant when the crack tip begins to propagate.

But the departure is indeed very small since it is found that the atomic positions are almost in the same with Figure 2. From the viewpoint of mechanics, the "seam" is like a type of initially disturbing force at the TB boundary. This disturbance tends to diffuse to every atom in MD and TB under the inter-atomic interaction, and causes them apart from their original positions. Without energy loss, these atoms vibrate around their equilibrium positions under the action of the atomic potential. These results clearly show that the numerical results are reasonable and the present scheme is stable and valid for both static and dynamic simulations.

To further verify the availability of dynamic simulation, the evolution of a crack tip in a Si slab (diamond structure) is simulated using the present multi-scale scheme under the condition of zero external force. Initially, the shape of crack is imposed as a rectangular cylinder. Figure 5a shows a part of the crack close to the right tip on the top view. It is found from the pure MD simulation that although all the atoms flutter around ideal lattice positions, the amplitude is too small in relation to the lattice spacing. The plots at different instants are almost the same with Figure 5a. In the application of the present multi-scale scheme, atoms around the tip are taken as TB atoms. The numerical result shows that the atoms near the crack tip move with time. Figure 5b shows the atomic positions at $t = 500$ time step and red solid circles represent the TB atoms. After that time, all the atoms begin vibrating around the positions shown in Figure 5b. It can be seen from the results obtained by two methods that for the atoms around a crack tip the quantum tight binding approximation is more reasonable and valid than the SW molecular dynamic approximation.

Based on the configuration shown in Figure 5b, a kind of tension along y-direction with the speed of 0.055 is simulated using the present scheme. Figure 6 gives the configuration of crack tip and y-component of force on atoms near the tip at the instant of $t = 8000\Delta t$. Figure 6a shows that the tip begins to propagate and the propagation may not be straight. It can be seen from the force shown in Figure 6b that the force on the atoms forming the crack tip is much larger than the force on other atoms. The seam (force) due to the handshaking can not be observed clearly. This indicates that the influence of the present seam on dynamic simulation is small.

5 Concluding remarks

In this paper, a new handshake scheme is presented for a tight-binding/molecular-dynamics multi-scale simulation of covalent crystals. In the present scheme, when

calculating the forces of MD atoms in the handshake region, the adjacent TB atoms are treated as 'MD' atoms. The computation of the whole MD subsystem is thus seamless. The same procedure is also used to calculate the repulsive force of TB atoms. To determine the electronic states of TB subsystem, hybrid orbitals are taken as basic atomic orbitals no matter whether the orbital belongs to the TB atom or the MD atom in the handshake region. The present handshaking avoids computing the physical parameters encountered due to introducing a new orbital model. Although there is still a small seam for the TB atoms in the handshake region, its magnitude decreases by around one order of magnitude compared to the old scheme. Dynamic simulation shows that the evolution of structure is reasonable and the present scheme is stable.

Appendix A: the present H and S matrices

In Section 2, a rough discussion has been made for Hamiltonian and non-orthogonality integrals. For the convenience of understanding and computing, a more detailed discussion is now presented.

For the sake of simplicity in description, we introduce a symbol

$$\begin{aligned} \Pi^{+} &= \lfloor (|\psi_{11}\rangle, |\psi_{12}\rangle, \cdots, |\psi_{N_1 N_\alpha}\rangle), \\ &\quad \times (|\psi_1\rangle, |\psi_2\rangle, \cdots, |\psi_L\rangle) \rfloor \\ &= \left[\Pi^{+}(\mathrm{I}), \Pi^{+}(\mathrm{L})\right], \end{aligned} \tag{A.1}$$

as an ensemble vector of all hybrid orbitals in equation (5), where superscript "+" denotes transposition. After applying the variational principle to equations (4) and (5), the energy E in (4) and coefficients in (5) satisfy,

$$\begin{bmatrix} \Pi(\mathrm{I}) H \Pi^{+}(\mathrm{I}), \Pi(\mathrm{I}) H \Pi^{+}(\mathrm{L}) \\ \Pi(\mathrm{L}) H \Pi^{+}(\mathrm{I}), \Pi(\mathrm{L}) H \Pi^{+}(\mathrm{L}) \end{bmatrix} = \mathrm{E} \begin{bmatrix} \Pi(\mathrm{I}) \Pi^{+}(\mathrm{I}), \Pi(\mathrm{I}) \Pi^{+}(\mathrm{L}) \\ \Pi(\mathrm{L}) \Pi^{+}(\mathrm{I}), \Pi(L) \Pi^{+}(\mathrm{L}) \end{bmatrix} \begin{bmatrix} C_{\mathrm{I}} \\ C_{\mathrm{L}} \end{bmatrix}. \tag{A.2}$$

By comparison with equation (7), we have,

$$\begin{aligned} H_{\mathrm{II}} &= \Pi(\mathrm{I}) H \Pi^{+}(\mathrm{I}) = \{\langle\psi_{i\alpha}| H |\psi_{j\beta}\rangle\} \\ H_{\mathrm{IL}} &= \Pi(\mathrm{I}) H \Pi^{+}(\mathrm{L}) = \{\langle\psi_{i\alpha}| H |\psi_{l}\rangle\} \\ H_{\mathrm{LI}} &= \Pi(\mathrm{L}) H \Pi^{+}(\mathrm{I}) = \{\langle\psi_{l}| H |\psi_{j\beta}\rangle\} \\ H_{\mathrm{LL}} &= \Pi(\mathrm{L}) H \Pi^{+}(\mathrm{L}) = \{\langle\psi_{l}| H |\psi_{l}\rangle\}, \end{aligned} \tag{A.3}$$

and

$$\begin{aligned} S_{\mathrm{II}} &= \Pi(\mathrm{I}) \Pi^{+}(\mathrm{I}) = \{\langle\psi_{i\alpha}|\psi_{j\beta}\rangle\} \\ S_{\mathrm{IL}} &= \Pi(\mathrm{I}) \Pi^{+}(\mathrm{L}) = \{\langle\psi_{i\alpha}|\psi_{l}\rangle\} \\ S_{\mathrm{LI}} &= \Pi(\mathrm{L}) \Pi^{+}(\mathrm{I}) = \{\langle\psi_{l}|\psi_{j\beta}\rangle\} \\ S_{\mathrm{LL}} &= \Pi(\mathrm{L}) \Pi^{+}(\mathrm{L}) = \{\langle\psi_{l}|\psi_{l}\rangle\}. \end{aligned} \tag{A.4}$$

It has been pointed out in Sections 2 and 3 that both $|\psi_{i\alpha}\rangle$ and $|\psi_{l}\rangle$ are taken as the hybrid orbitals given by equation (6). Since the hybrid orbital is a linear superposition of four atomic orbitals, any matrix element in (A.3) is a linear superposition of the following expressions.

$$\langle s_i| H |s_j\rangle, \langle s_i| H |p_{x,j}\rangle, \langle p_{x,i}| H |p_{x,j}\rangle, \langle p_{x,i}| H |p_{y,j}\rangle, \langle p_{x,i}| H |p_{z,j}\rangle. \tag{A.5}$$

Similarly, any matrix element in (A.4) is a linear superposition of the following expressions,

$$\langle s_i \mid s_j\rangle, \ \langle s_i \mid p_{x,j}\rangle, \langle p_{x,i} \mid p_{x,j}\rangle, \langle p_{x,i} \mid p_{y,j}\rangle, \langle p_{x,i} \mid p_{z,j}\rangle. \tag{A.6}$$

When $i = j$, the values of expressions in (A.5) and (A.6) can be obtained from text book.

$$\begin{aligned} \langle s_i| H |s_i\rangle = E_{\mathrm{s}}, \ \langle p_{x,i}| H |p_{x,i}\rangle = E_p \\ \langle s_i| H |p_{x,i}\rangle = \langle p_{x,i}| H |p_{y,i}\rangle = \langle p_{x,i}| H |p_{x,i}\rangle = 0 \end{aligned}$$

$$\begin{aligned} \langle s_i \mid s_i\rangle = \langle p_{x,i} \mid p_{x,i}\rangle = 1 \\ \langle s_i \mid p_{x,i}\rangle = \langle p_{x,i} \mid p_{y,i}\rangle = \langle p_{x,i} \mid p_{z,i}\rangle = 0. \end{aligned}$$

When $i \neq j$, the expressions in (A.5) and (A.6) deal with the hopping integrals of two atomic orbitals which belong to two different atoms. According to the non-orthogonal tight binding model based on the two-center integral approximation [15], if the two atoms are not neighbors, the values of these expressions are zero. If the two atoms are neighbors, the values of expressions (A.5) are fully determined by four independent integrals, $V(ss\sigma)$, $V(sp\sigma)$, $V(pp\sigma)$ and $V(pp\pi)$, while the values of expressions (A.6) can be determined by the extended Hückel theory. The more detail discussion can be found in references [15,16] for the non-orthogonal tight binding model based on the two-center integral approximation.

At present, $\langle\psi_{i\alpha}| H |\psi_{j\beta}\rangle$ is taken as an example to show how to calculate the matrix elements. For the case of $i = j$, it is easy to obtain

$$\langle\psi_{i\alpha}| H |\psi_{j\beta}\rangle = [\alpha_s\beta_s E_s + (\alpha_x\beta_x + \alpha_y\beta_y + \alpha_z\beta_z)E_p]\,\delta_{\alpha\beta} \tag{A.7}$$

$$\langle\psi_{i\alpha} \mid \psi_{i\beta}\rangle = \delta_{\alpha\beta}. \tag{A.8}$$

For the case of $i \neq j$, the key is to find $\langle\psi_{i\alpha}|H|\psi_{j\beta}\rangle_{\perp}$ corresponding to orthogonal tight binding model. From the reference [16] (pp. 145–149), it can be derived that

$$\begin{aligned} \langle\psi_{i\alpha}(\boldsymbol{r}_i)| H |\psi_{j\beta}(\boldsymbol{r}_j)\rangle_{\perp} &= \alpha_s\beta_s V(ss\sigma) + (\alpha_x\beta_x + \alpha_y\beta_y \\ &\quad + \alpha_z\beta_z) V(pp\pi) + [\alpha_s(\beta_x l_x + \beta_y l_y + \beta_z l_z) \\ &\quad - \beta_s(\alpha_x l_x + \alpha_y l_y + \alpha_z l_z)] V(sp\sigma) + (\alpha_x l_x \\ &\quad + \alpha_y l_y + \alpha_z l_z)(\beta_x l_x + \beta_y l_y + \beta_z l_z)[V(pp\sigma) - V(pp\pi)] \end{aligned} \tag{A.9}$$

where $(l_x, l_y, l_z) = \boldsymbol{r}_j - \boldsymbol{r}_i)/|\boldsymbol{r}_j - \boldsymbol{r}_i|$.

References

1. N.J. Wagner, B.L. Holian, A.F. Voter, Phys. Rev. A **45**, 8457 (1992)
2. F.F. Abraham, Europhys. Lett. **38**, 103 (1997)
3. F.F. Abraham, J.Q. Broughton, Comput. Mater. Sci. **10**, 1 (1998)
4. M.L. Falk, J.S. Langer, Phys. Rev. E **57**, 7192 (1998)
5. M.L. Falk, Phys. Rev. B **60**, 7062 (1999)
6. C.L. Rountree, R.K. Kalia, E. Lidorikis, A. Nakano, L.V. Brutzel, P. Vashishta, Annu. Rev. Mater. Res. **32**, 377 (2002)
7. F.F. Abraham, J.Q. Broughton, N. Bernstein, E. Kaxiras, Europhys. Lett. **44**, 783 (1998)
8. F.F. Abraham, Int. J. Modern Phys. C **11**, 1135 (2000)
9. F.F. Abraham, Nucl. Instr. and Meth. in Phys. Res. B **180**, 72 (2001)
10. J.Q. Broughton, F.F. Abraham, N. Bernstein, E. Kaxiras, Phys. Rev. B **60**, 2391 (1999)
11. R.E. Rudd, J.Q. Broughton, Phys. Stat. Sol. (b) **217**, 251 (2000)
12. N. Bernstein, D. Hess, Mat. Res. Soc. Symp. Proc. **653**, Z2.7.1 (2001)
13. S. Ogata, F. Shimojo, R.K. Kalia, S. Nakano, P. Vashishta, Comp. Phys. Comm. **149**, 30 (2002)
14. F.H. Stillinger, T.A. Weber, Phys. Rev. B **31**, 5262 (1985)
15. N. Bernstein, E. Kaxiras, Phys. Rev. B **56**, 10488 (1997)
16. G. Grosso, G.P. Parravicini, *Solid State Physics* (Academic Press, 2000)